



Macroscopic Traffic Flow Characterization at Bottlenecks

Amir Iftikhar ^a, Zawar H. Khan ^{a, b*}, T. Aaron Gulliver ^c, Khurram S. Khattak ^d,
Mushtaq A. Khan ^e, Murtaza Ali ^e, Nasru Minallahe ^d

^a National Institute of Urban Infrastructure Engineering, Peshawar, Pakistan.

^b Department of Electrical Engineering, University of Engineering & Technology Peshawar, Pakistan.

^c Department of Electrical and Computer Engineering, University of Victoria, PO Box 1700, STN CSC, Victoria, Canada.

^d Department of Computer System Engineering, University of Engineering & Technology Peshawar, Pakistan.

^e Department of Electrical Engineering, University of Engineering & Technology Mardan, Pakistan.

Received 19 December 2019; Accepted 16 May 2020

Abstract

Traffic congestion is a significant issue in urban areas. Realistic traffic flow models are crucial for understanding and mitigating congestion. Congestion occurs at bottlenecks where large changes in density occur. In this paper, a traffic flow model is proposed which characterizes traffic at the egress and ingress to bottlenecks. This model is based on driver response which includes driver reaction and traffic stimuli. Driver reaction is based on time headway and driver behavior which can be classified as sluggish, typical or aggressive. Traffic stimuli are affected by the transition width and changes in the equilibrium velocity distribution. The explicit upwind difference scheme is used to evaluate the Lighthill, Whitham, and Richards (LWR) and proposed models with a continuous injection of traffic into the system. A stability analysis of these models is given and both are evaluated over a road of length 10 km which has a bottleneck. The results obtained show that the behavior with the proposed model is more realistic than with the LWR model. This is because the LWR model cannot adequately characterize driver behavior during changes in traffic flow.

Keywords: Macroscopic Traffic Model; Traffic Flow; Transition; LWR Model; Explicit Upwind Difference Scheme; Stability Analysis.

1. Introduction

Traffic congestion is a critical issue in urban areas around the world [1] and it is getting worse. The Traffic Index (TI) is a composite index of the time to journey from home to work [2]. The 2017 TI indicates that congestion levels in Mexico City, Bangkok, Jakarta, Istanbul, and Beijing were 66%, 61%, 58%, 49%, and 46%, respectively [3]. According to the INRIX report [1], congestion costs in the UK were approximately £8 billion in 2018 which is over £1,300 per driver. Further, an average UK road user spent 178 h in congestion in 2018 [4]. Congestion occurs when there are traffic bottlenecks due to lane reductions, poor traffic light timing, accidents, and sharp curves. Bottlenecks can be recurring or nonrecurring. Recurring bottlenecks appear at the same time of day and day of the week, whereas nonrecurring bottlenecks appear randomly and are typically due to conditions such as accidents, precipitation and/or poor visibility [5]. In order to mitigate congestion, it is necessary to understand traffic behavior and characterize it realistically [6]. Transitions are large changes in density which can occur at the egress or ingress to a road or at lane reductions and can cause bottlenecks [7]. A traffic model based on driver response is required which characterizes traffic behavior during transitions. This can be employed to mitigate congestion and decrease travel time [6].

* Corresponding author: zawarkhan@nwfpuet.edu.pk

 <http://dx.doi.org/10.28991/cej-2020-03091543>



© 2020 by the authors. Licensee C.E.J, Tehran, Iran. This article is an open access article distributed under the terms and conditions of the Creative Commons Attribution (CC-BY) license (<http://creativecommons.org/licenses/by/4.0/>).

Traffic flow can be homogeneous or heterogeneous and equilibrium or non-equilibrium. Homogeneous flow corresponds to similar vehicle velocities and densities so that the headway is constant [8]. Time headway is the time required for vehicle alignment and is necessary to avoid accidents [9]. The distance headway is between the rear bumpers of consecutive vehicles and is covered during the time headway [11]. Driver response is slow for a large time headway and interactions between vehicles are low, whereas with a small time headway the interactions are high. In a heterogeneous flow, velocities and densities vary so that the headways between vehicles differ [12]. Lane discipline exists in a homogeneous flow, but typically not in heterogeneous traffic [13]. Further, a heterogeneous flow is not based on the first in first out rule [14]. Equilibrium flow decreases with increasing density, but a non-equilibrium flow is often not density dependent [15]. In a non-equilibrium flow, changes in traffic occur due to different driver perceptions and reactions [12] which vary with age, ethnicity, memory, location, and experience [7].

Traffic flow models can be categorized as microscopic, macroscopic or mesoscopic. Microscopic models characterize individual vehicle behavior based on their interactions. They are used to investigate the temporal and spatial behavior of vehicles based on interactions within a small area. Macroscopic models consider the aggregate behavior of traffic using parameters such as headway, driver response, density, velocity and flow [37-39]. Mesoscopic models incorporate characteristics of both microscopic and macroscopic models [10]. For example, vehicles are modeled at an individual level and the general behavior is evaluated. Examples include cluster, headway distribution and flow emission models [16]. Macroscopic models have low computational complexity [7, 40] and have been shown to provide good performance [12, 37-42], so these models are considered here.

Lighthill, Witham, and Richards (LWR) developed a macroscopic traffic flow model based on the law of conservation. This model considers the relationship between traffic density and flow [17]. It is assumed that small changes in traffic occur such that vehicles align their speeds in zero time [15], which can result in sharp changes in flow over small distances [18, 19]. The LWR model is commonly employed due to its simplicity [22], but it ignores the headway during alignment at transitions [21, 22] which causes unrealistic changes in flow. To improve the LWR model, Wong proposed including driver behavior [20] such as the velocity distribution. However, this model assumes that faster vehicles overcome slower vehicles during congestion which is typically not possible. Helbing considered lane discipline while characterizing changes in traffic [21] but not changes in velocity, so it is inadequate [13]. Newell improved the LWR model by incorporating stop and go traffic behavior. While this model includes changes in density, it does not consider the distances between vehicles for alignment [7, 41]. Michalopoulos and Kuhne [22] incorporated ramps by using source terms with the LWR model, but traffic changes due to transitions are ignored [23].

In this paper, a new model is proposed to characterize traffic changes at transitions due to bottlenecks. This model considers changes in velocity based on driver reaction and traffic stimuli. Driver reaction is introduced as a function of time headway to characterize sluggish, typical and quick driver behavior. These reactions are due to traffic stimuli, i.e. a decrease in velocity as vehicles move towards a bottleneck or an increase at the egress from a bottleneck. The explicit upwind difference scheme is used to approximate the LWR and proposed models with a continuous injection of traffic into the system. The performance of these models is evaluated over a road of length 10 km which has a bottleneck.

The remainder of this paper is organized as follows. Section 2 presents the LWR and proposed models and the explicit upwind difference scheme is used in Section 3 to approximate these models. A stability analysis of the LWR and proposed models is given in Section 4, and their performance is compared in Section 5. Finally, some concluding remarks are given in Section 6.

2. Traffic Flow Models

The Lighthill, Whitham, and Richards (LWR) model [22] is based on vehicle conservation. It assumes a long infinite road with small changes in flow [15, 24]. The LWR model is given by [25]:

$$\frac{\partial \rho}{\partial t} + \frac{\partial \rho v}{\partial x} = 0 \quad (1)$$

and Equation 1 can be written as [26]:

$$\frac{\partial \rho}{\partial t} + c \frac{\partial \rho}{\partial x} = 0 \quad (2)$$

With;

$$c = \frac{dx}{dt} \quad (3)$$

Which is analogous to $q'(\rho)$ [7, 25, 26]. The flow is:

$$q(\rho) = \rho v(\rho)$$

so that;

$$q'(\rho) = \frac{\partial \rho v(\rho)}{\partial \rho}$$

Then Equation 1 can be expressed as:

$$\frac{\partial \rho}{\partial t} + q'(\rho) \frac{\partial \rho}{\partial x} = 0 \tag{4}$$

The equilibrium velocity distribution $v(\rho)$ is a function of density and is the target when a transition occurs [7]. The most commonly used distribution is from Greenshields [29] and is given by:

$$v(\rho) = v_m \left(1 - \frac{\rho}{\rho_m}\right) \tag{5}$$

Where v_m is the maximum velocity and ρ_m is the maximum density. According to this model, traffic moves faster at lower densities. This distribution is employed here due to its simplicity and extensive use in characterizing traffic behavior. Taking the derivative with respect to density gives;

$$\frac{dv(\rho)}{d\rho} = \frac{d}{d\rho} \left(v_m \left(1 - \frac{\rho}{\rho_m}\right) \right) = -\frac{v_m}{\rho_m} \tag{6}$$

This is the stimulus for a driver and is a function of the maximum velocity. Only the magnitude of the stimulus from (6) is required, so we employ:

$$\left| \frac{dv(\rho)}{d\rho} \right| = \left| \frac{v_m}{\rho_m} \right| \tag{7}$$

The alignment in velocity Δv due to a stimulus occurs during the time headway τ [7] so that:

$$\Delta v = a\tau \tag{8}$$

Where a is the driver response. Further, Δv is the change in velocity to achieve equilibrium which gives:

$$\Delta v = v - v(\rho) \tag{9}$$

Substituting (9) in (8), we have:

$$v - v(\rho) = a\tau \tag{10}$$

or

$$v = a\tau + v(\rho) \tag{11}$$

The transition width δt is defined as the difference between preceding and forward densities and characterizes the change in traffic density. It is based on the road geometry, i.e. when a lane is reduced the density increases and vice versa. For a small δt , small changes in velocity occur and the flow is smoother while for a large δt , the changes in velocity are large and can become oscillatory. The driver stimulus is given by:

$$\frac{1}{\delta t} \frac{dv(\rho)}{d(\rho)} \tag{12}$$

Driver reaction to a forward stimulus varies according to age, gender, ethnicity, and experience [7]. The time taken by a driver to observe and react is the physiological response [12]. The time to align is based on this response [29] and can be characterized by the time headway [29]. A sluggish driver takes longer than a typical driver to align, whereas an aggressive driver is quicker. The physiological response can be expressed as:

$$b = \frac{\tau}{\tau_p} \tag{13}$$

Where τ_p is the time headway for a typical driver. Driver behavior is aggressive when $b < 1$, typical when $b = 1$, and sluggish for $b > 1$. The driver response [29] is the product of stimuli and reaction, so from (12) and (13) we have:

$$a = \frac{1}{\delta t} \left| \frac{dv(\rho)}{d\rho} \right| \frac{\tau}{\tau_p} \tag{14}$$

Substituting Equation 14 in Equation 11 gives:

$$v = v(\rho) + \frac{1}{\delta t} \left| \frac{dv(\rho)}{d(\rho)} \right| b\tau \tag{15}$$

Congestion is mitigated when this velocity is greater than $v(\rho)$, i.e. when there is egress from a bottleneck. The velocity is less than $v(\rho)$ if there is ingress to a bottleneck so

$$v = v(\rho) \pm \frac{1}{\delta t} \left| \frac{dv(\rho)}{d(\rho)} \right| b\tau \tag{16}$$

Substituting Equation 16 in the LWR model Equation 4, the proposed model for egress from a bottleneck is:

$$\frac{\partial \rho}{\partial t} + \left(\rho v(\rho) + \rho \frac{1}{\delta t} \left| \frac{dv(\rho)}{d(\rho)} \right| b\tau \right)' \frac{\partial \rho}{\partial x} = 0 \tag{17}$$

and for ingress is:

$$\frac{\partial \rho}{\partial t} + \left(\rho v(\rho) - \rho \frac{1}{\delta t} \left| \frac{dv(\rho)}{d(\rho)} \right| b\tau \right)' \frac{\partial \rho}{\partial x} = 0 \tag{18}$$

This model characterizes traffic changes based on velocity and forward conditions. It reduces to the LWR model when there is no change in traffic conditions ahead such that:

$$\frac{dv(\rho)}{d(\rho)} = 0$$

3. Model Evaluation

The explicit upwind difference scheme is employed to approximate the proposed and LWR models. This scheme has lower complexity than the Godunov and FORCE schemes [30, 31]. It employs the forward difference in time and the backward difference in space [32]. A road is considered with M equidistant road segments and N equal duration time steps. The total length of the road is x_m and the total time duration is t_m , so that $\Delta t = t_m/N$ and $\Delta x = x_m/M$. The traffic density at the n -th time step in the i -th road segment is:

$$\frac{\partial \rho}{\partial t} = \frac{\rho_i^{n+1} - \rho_i^n}{t_{n+1} - t_n} \tag{19}$$

and the corresponding traffic flow is:

$$\frac{\partial q}{\partial x} = \frac{q_i^n - q_{i-1}^n}{x_i - x_{i-1}} \tag{20}$$

Substituting $q = \rho v$ gives:

$$\frac{\partial q}{\partial x} = \frac{(\rho v)_i^n - (\rho v)_{i-1}^n}{x_i - x_{i-1}} \tag{21}$$

The LWR model can be discretized as:

$$\frac{\rho_i^{n+1} - \rho_i^n}{t_{n+1} - t_n} + \frac{(\rho v)_i^n - (\rho v)_{i-1}^n}{x_i - x_{i-1}} = 0 \tag{22}$$

and substituting $\Delta t = t_{n+1} - t_n$ and $\Delta x = x_{i+1} - x_i$ gives:

$$\rho_i^{n+1} = \rho_i^n + \frac{\Delta t}{\Delta x} ((\rho v)_{i-1}^n - (\rho v)_i^n) \tag{23}$$

The density update in segment i for time step $n + 1$ is:

$$\rho_i^{n+1} = \rho_i^n + q'(\rho_i^n) \frac{\Delta t}{\Delta x} [(\rho)_{i-1}^n - (\rho)_i^n] \tag{24}$$

The corresponding density update for the proposed model is:

$$\rho_i^{n+1} = \rho_i^n + \left(\rho_i^n v(\rho_i^n) \pm \rho_i^n \left| \frac{\partial v(\rho_i^n)}{\partial \rho_i^n} \right| \frac{b\tau}{\delta t} \right)' \frac{\Delta t}{\Delta x} [(\rho)_{i-1}^n - (\rho)_i^n] \tag{25}$$

4. Stability Analysis

A finite difference scheme is consistent if the discretization error tends to zero, in which case the numerical solution is stable and convergent [33]. This requires that the Courant-Friedrichs-Lewy (CFL) condition is satisfied [15]. The error at the $(n + 1)$ -th time step should be less than the error at the n -th time step for segment i so that:

$$|\gamma_i^{n+1}| < |\gamma_i^n| \tag{26}$$

and since there are a finite number of vehicles:

$$|\rho_i^{n+1}| < |\rho_i^n| \tag{27}$$

The density ρ_i^n can be expressed as [33]:

$$\rho_i^n = \sum_{k=-\infty}^{\infty} e_k^{\alpha n} e^{jkx_i} \tag{28}$$

Where $j = \sqrt{-1}$, $e_k^{\alpha n}$ is the k -th Fourier component, and $e^{jkx_i} = \cos kx_i + j \sin kx_i$. Substituting this in Equation 27 gives:

$$|e_k^{n+1} e^{jkx_i}| < |e_k^n e^{jkx_i}| \tag{29}$$

Or:

$$B = \left| \frac{e_k^{n+1}}{e_k^n} \right| < 1 \tag{30}$$

Where B is the density factor. Substituting ρ_i^n from Equation 28 in 24 gives:

$$\sum_{k=-\infty}^{\infty} e^{\alpha(n+i)} e^{jk_m x} = \sum_{k=-\infty}^{\infty} e^{\alpha n} e^{jk_m x} - q'(\rho) \frac{\Delta t}{\Delta x} \left[\sum_{k=-\infty}^{\infty} e^{\alpha n} e^{jk_m x} - \sum_{k=-\infty}^{\infty} e^{\alpha n} e^{jk_m(x-i)} \right] \tag{31}$$

and considering the k -th term:

$$e^{\alpha(n+i)} e^{jk_m x} = e^{\alpha n} e^{jk_m x} - q'(\rho) \frac{\Delta t}{\Delta x} \left[e^{\alpha n} e^{jk_m x} - e^{\alpha n} e^{jk_m(x-i)} \right] \tag{32}$$

For simplicity, let:

$$C = q'(\rho) \frac{\Delta t}{\Delta x} \tag{33}$$

and dividing both sides by $e_k^{\alpha n} e^{jk_m x}$ gives:

$$B = e^{\alpha \Delta t} = 1 - C[1 - e^{-jk \Delta x}] \tag{34}$$

Using $e^{-jk \Delta x} = \cos k \Delta x - j \sin k \Delta x$, this becomes:

$$B = 1 - C[1 - \cos(k \Delta x)] - jC \sin(k \Delta x) \tag{35}$$

The numerical scheme is stable if the magnitude of B is less than 1. We have that;

$$\begin{aligned} B^2 &= (1 - C[1 - \cos(k \Delta x)])^2 + C^2 \sin^2(k \Delta x), \\ &= 1 - 2C[1 - \cos(k \Delta x)] + C^2[1 - \cos(k \Delta x)]^2 + C^2 \sin^2(k \Delta x), \\ &= 1 - 2C[1 - \cos(k \Delta x)] + C^2[1 - 2\cos(k \Delta x) + \cos^2(k \Delta x)] + C^2 \sin^2(k \Delta x), \\ &= 1 - 2C[1 - \cos(k \Delta x)] + C^2 - 2C^2 \cos(k \Delta x) + C^2 \cos^2(k \Delta x) + C^2 \sin^2(k \Delta x), \\ &= 1 - 2C[1 - \cos(k \Delta x)] + C^2 - 2C^2 \cos(k \Delta x) + C^2[\cos^2(k \Delta x) + \sin^2(k \Delta x)], \end{aligned} \tag{36}$$

and substituting $\cos^2(k \Delta x) + \sin^2(k \Delta x) = 1$, this becomes;

$$\begin{aligned} B^2 &= 1 - 2C[1 - \cos(k \Delta x)] + C^2 - 2C^2 \cos(k \Delta x) + C^2, \\ &= 1 - 2C[1 - \cos(k \Delta x)] + 2C^2 - 2C^2 \cos(k \Delta x), \\ &= 1 - 2C[1 - \cos(k \Delta x)] + 2C^2[1 - \cos(k \Delta x)], \\ &= 1 + [1 - \cos(k \Delta x)](-2C + 2C^2), \\ &= 1 - 2C[1 - \cos(k \Delta x)](1 - C). \end{aligned} \tag{37}$$

The technique is stable if $B^2 < 1$ which gives;

$$1 - 2C[1 - \cos(k \Delta x)](1 - C) < 1 \tag{38}$$

Or:

$$-2C[1 - \cos(k \Delta x)](1 - C) < 0 \tag{39}$$

Since:

$$-1 \leq \cos(k \Delta x) \leq 1 \tag{40}$$

it is sufficient to find C such that:

$$1 - C > 0$$

or:

$$C < 1$$

Thus, the finite upwind difference scheme is stable if:

$$C < 1 \tag{41}$$

in which case the maximum distance covered in a time step Δt is less than the segment length Δx .

For the LWR model:

$$C = v_m \frac{\Delta t}{\Delta x} \tag{42}$$

If $C < 1$, the numerical scheme is stable and small changes in velocity will not cause large changes in traffic behavior [33, 34]. For the performance evaluation in the next section, the maximum velocity for both the proposed and LWR

models is $v_m = 20$ km/h. Choosing $\Delta t=0.0005$ h and $\Delta x=0.1$ km gives:

$$C = 20 \times \frac{0.0005}{0.1} = 0.10 < 1 \tag{43}$$

so the numerical solutions for the LWR model are stable.

For the proposed model:

$$q'(\rho) = \left(v(\rho) \pm \frac{1}{\delta t} \left| \frac{\partial v(\rho)}{\partial(\rho)} \right| b\tau \right)$$

and using (33) and (41), the stability condition is:

$$\left(v(\rho) \pm \frac{1}{\delta t} \left| \frac{\partial v(\rho)}{\partial(\rho)} \right| b\tau \right) \frac{\Delta t}{\Delta x} < 1 \tag{44}$$

This is satisfied when the distance covered during Δt is less than Δx . The maximum of $v(\rho)$ is v_m and using Equation 7 gives:

$$\left(v_m \pm \frac{1}{\delta t} \left| \frac{v_m}{\rho_m} \right| b\tau \right) \frac{\Delta t}{\Delta x} < 1 \tag{45}$$

For the performance evaluation $\rho_m = 1$, $\delta t = 0.028$ for smooth changes in density, $b = 0.5$, and $\tau = 3$ s (0.0008 h). Choosing $\Delta t = 0.0005$ h and $\Delta x = 0.1$ km results in:

$$\left(20 \pm \frac{1}{0.028} \left| \frac{20}{1} \right| 0.5 \times 0.0008 \right) \frac{0.0005}{0.1} = 0.1014, 0.0985 < 1 \tag{46}$$

and considering $\delta t = 0.02$ for sudden changes in density gives:

$$\left(20 \pm \frac{1}{0.02} \left| \frac{20}{1} \right| 0.5 \times 0.0008 \right) \frac{0.0005}{0.1} = 0.102, 0.098 < 1 \tag{47}$$

so the numerical solutions for the proposed model are stable.

Table 1. Simulation Parameters

Name	Parameter	Value
Space step	Δx	0.1 km
Equilibrium velocity distribution	$v(\rho)$	Greenshields distribution
Time step	Δt	0.0005 h
Maximum velocity	v_m	20 km/h
Length of road	x_m	10 km
CFL condition for the LWR model	$q(\rho)' \frac{\Delta t}{\Delta x}$	0.10
CFL conditions for the proposed model at the ingress to a bottleneck	$q'(\rho) \frac{\Delta t}{\Delta x}$	0.1002
CFL conditions for the proposed model at the egress from a bottleneck	$q'(\rho) \frac{\Delta t}{\Delta x}$	0.0998
Initial density	$\rho(x, t = 0)$	$2.3\sin(x) + 30$ veh/km
Maximum density	ρ_m	1
Transition width for smooth changes	δt	0.028
Transition width for sudden changes	δt	0.02
Driver behavior	b	0.5
Time headway	τ	0.0008 h

5. Performance Results

The performance of the proposed and LWR models is evaluated in this section for a traffic bottleneck. A traffic bottleneck occurs when the capacity of a road changes suddenly [35]. In the first scenario, vehicles enter a ramp from the highway which is the ingress to a bottleneck, while in the second scenario, vehicles enter the highway from a ramp which is the egress from a bottleneck. The LWR model is the same for both scenarios as this model cannot characterize bottleneck behavior.

The maximum density is $\rho_m = 1$ which indicates that 100% of the road is occupied with vehicles. For smooth changes in density, the bottleneck has transition width $\delta t = 0.028$ and for sudden changes in density, the bottleneck has transition width $\delta t = 0.02$. The boundary conditions are nonperiodic so that traffic enters the road at 0 km and

leaves at 10 km. The total simulation time is $t_m = 60$ s, the time headway is $\tau = 3$ s [36], and $b = 0.5$ which denotes aggressive behavior. The maximum velocity is $v_m = 20$ km/h and traffic adjusts to the Greenshields equilibrium distribution (5) when a change occurs [34]. The initial density distribution is a periodic function [32]:

$$\rho = 2.3\sin(x) + 30 \tag{48}$$

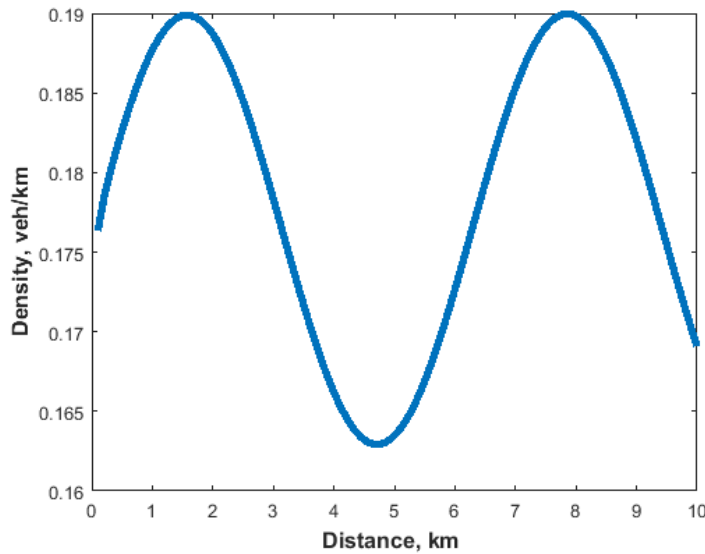


Figure 1. The proposed model density behavior at the ingress to a ramp from a highway at 1 s.

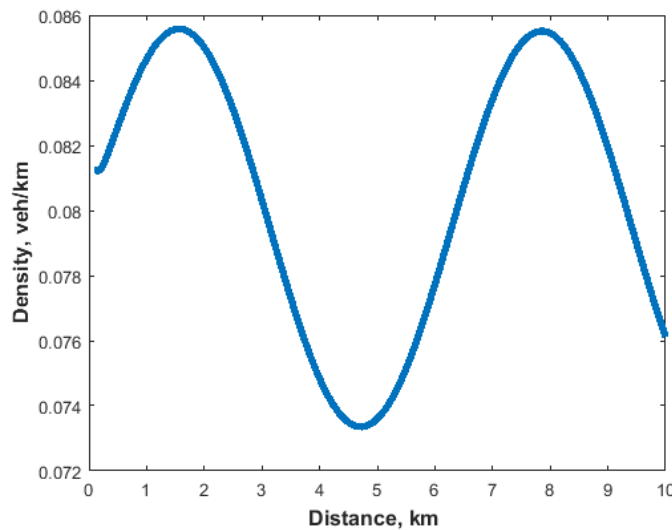


Figure 2. The proposed model density behavior at the egress from a ramp to a highway at 1 s.

Figure 1 shows the normalized traffic density behavior with the proposed model at the ingress to a ramp from a highway at 1 s. The density is 0.176 veh/km at 0.1 km, increases to 0.190 veh/km at 1.5 km, and then decreases to 0.163 veh/km at 4.6 km. At 7.8 km, the density is 0.190 veh/km and decreases to 0.169 veh/km at 10 km. Figure 2 shows the corresponding behavior at the egress from a ramp to a highway at 1 s. The density is 0.081 veh/km at 0.1 km, increases to 0.086 veh/km at 1.5 km, and then decreases to 0.074 veh/km at 4.6 km. At 7.8 km, the density is 0.086 veh/km and decreases to 0.076 veh/km at 10 km.

Figure 3 shows the normalized density behavior with the proposed model at the ingress to a ramp from a highway at 10 s. The density is 0.163 veh/km at 0.1 km, increases to 0.189 veh/km at 1.5 km, and then decreases to 0.163 veh/km at 4.6 km. At 7.8 km the density is 0.190 veh/km and decreases to 0.169 veh/km at 10 km. Figure 4 shows the corresponding behavior at the egress from a ramp to a highway at 10 s. At 0 km, the density is 0.092 veh/km, decreases to 0.086 veh/km at 0.5 km, and then increases to 0.087 veh/km at 1.5 km. The density is 0.073 veh/km at 4.7 km and increases to 0.086 veh/km at 7.9 km. At 10 km, the density is 0.077 veh/km. Figure 5 shows the density behavior with the LWR model at the egress or ingress from a highway at 10 s. At 0 km, the density is 0.036 veh/km, increases to 0.038 veh/km at 1.5 km, and then decreases to 0.033 veh/km at 4.7 km. The density is 0.038 veh/km at 7.8 km and decreases to 0.034 veh/km at 10 km.

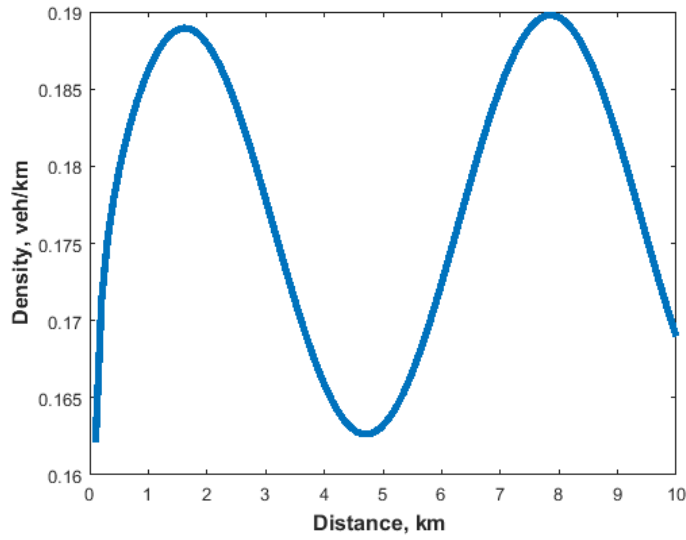


Figure 3. The proposed model density behavior at the ingress to a ramp from a highway at 10 s.

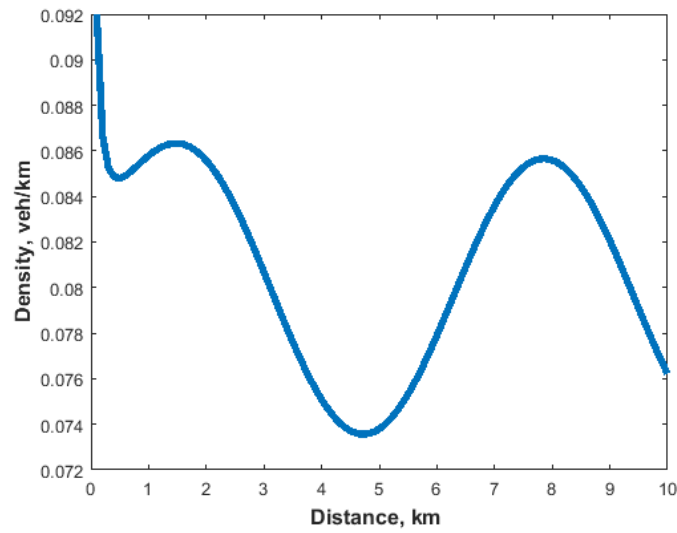


Figure 4. The proposed model density behavior at the egress from a ramp to a highway at 10 s.

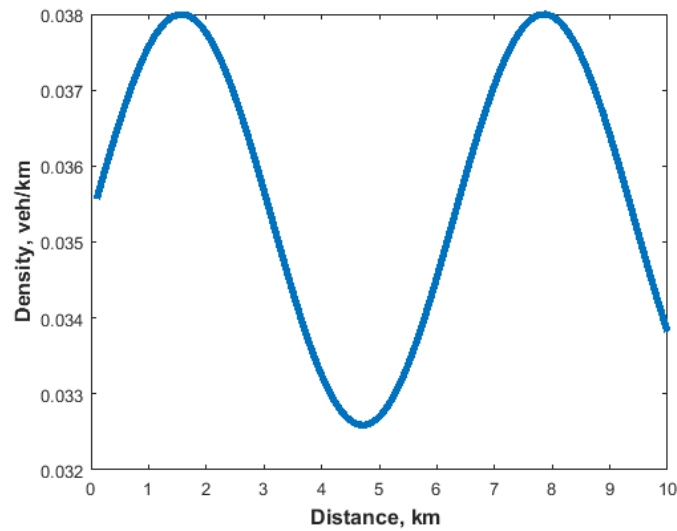


Figure 5. The density behavior at 10 s with the LWR model at the egress or ingress from a highway.

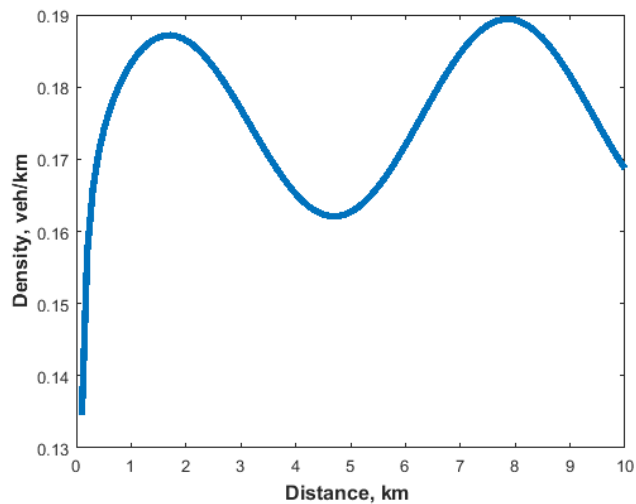


Figure 6. The proposed model density behavior at the ingress to a ramp from a highway at 20 s.

Figure 6 shows the normalized density behavior of the proposed model at the ingress to a ramp from a highway at 20 s. The normalized density is 0.135 veh/km at 0.1 km, and increases to 0.187 veh/km at 1.5 km. The density then decreases to 0.165 veh/km at 4.6 km. At 7.8 km the density is 0.190 veh/km and decreases to 0.170 veh/km at 10 km. Figure 7 presents the corresponding behavior at the egress from a ramp to a highway at 20 s. At 0 km, the density is 0.140 veh/km. The density decreases to 0.095 veh/km at 0.5 km, and then to 0.073 veh/km at 4.7 km. It increases to 0.086 veh/km at 7.9 km and decreases to 0.078 veh/km at 10 km. Figure 8 shows the normalized density behavior of the LWR model at the ingress or egress from a highway at 50 s. At 0 km the normalized density is 0.071 veh/km, increases to 0.076 veh/km at 1.5 km, and then decreases to 0.065 veh/km at 4.7 km. The density increases to 0.076 veh/km at 7.8 km and then decreases to 0.068 veh/km at 10 km.

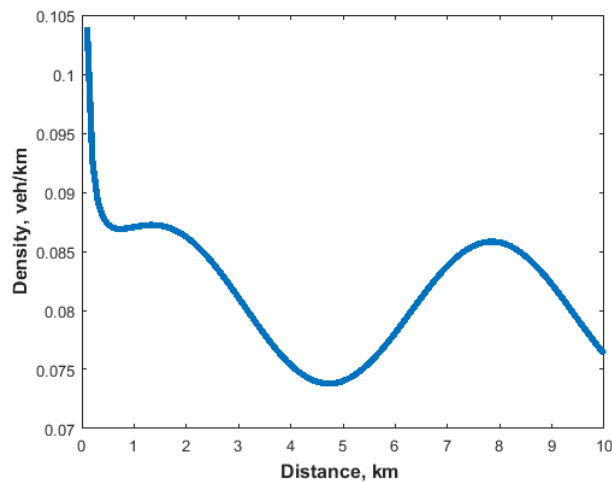


Figure 7. The proposed model density behavior at the egress from a ramp to a highway at 20 s.

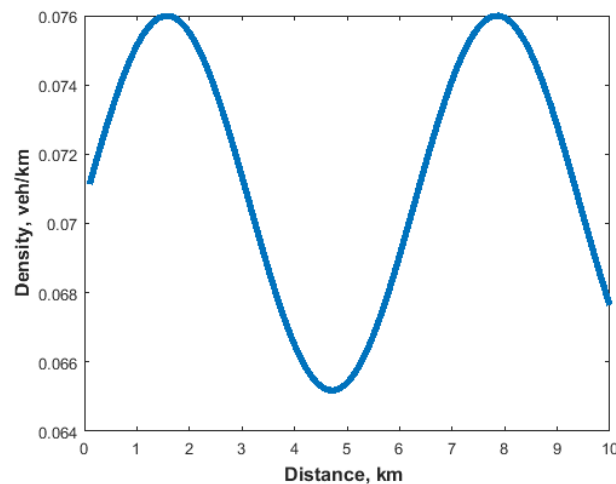


Figure 8. The density behavior at 20 s with the LWR model at the ingress or egress from a highway.

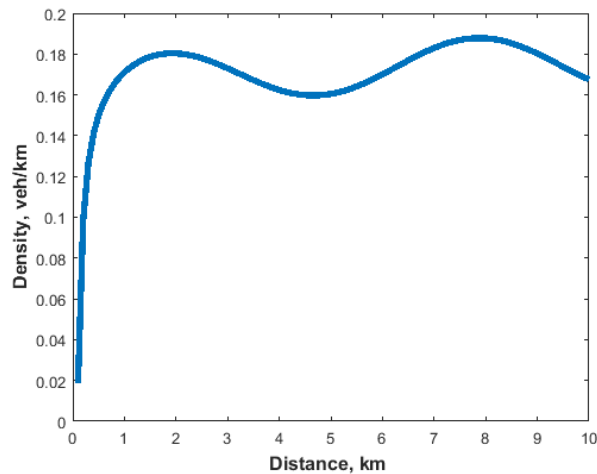


Figure 9. The proposed model density behavior at the ingress to a ramp from a highway at 50 s.

Figure 9 shows the normalized density behavior of the proposed model at 50 s at the ingress to a ramp from a highway. At 0.1 km, the density is 0.010 veh/km which increases to 0.178 veh/km at 1.8 km. The density decreases to 0.160 veh/km at 4.6 km, increases to 0.182 veh/km at 7.9 km, and then decreases to 0.163 veh/km at 10 km. Figure 10 presents the corresponding behavior at the egress from a ramp to a highway at 50 s. At 0 km, the density is 0.150 veh/km, decreases to 0.094 veh/km at 1.5 km, and then decreases to 0.075 veh/km at 4.7 km. The density increases to 0.087 veh/km at 7.9 km and then decreases to 0.078 veh/km at 10 km. Figure 11 shows the normalized density behavior of the LWR model at the ingress or egress from a highway at 50 s. At 0.1 km, the density is 0.176 veh/km and then increases to 0.187 veh/km at 1.5 km. It decreases to 0.162 veh/km at 4.7 km, increases to 0.188 veh/km at 7.8 km, and then decreases to 0.168 veh/km at 10 km.

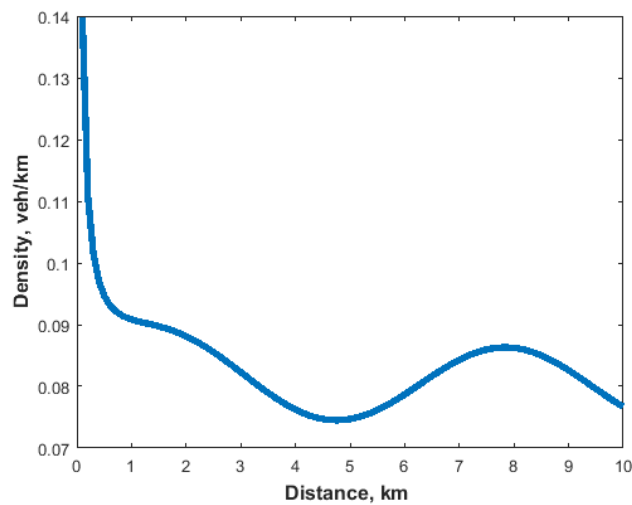


Figure 10. The proposed model density behavior at the egress from a ramp to a highway at 50 s.

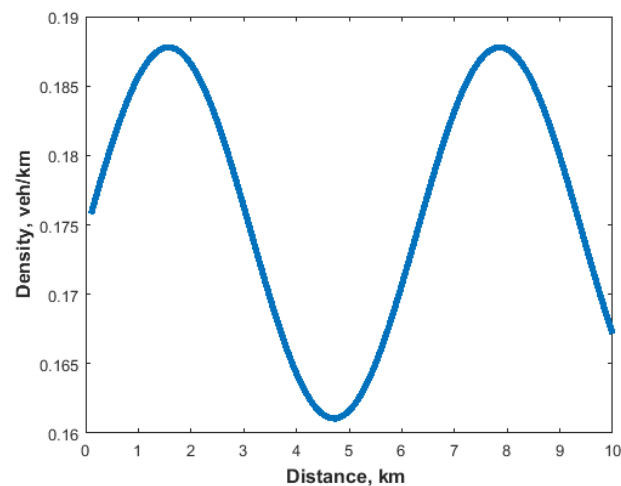


Figure 11. The density behavior at 50 s with the LWR model at the ingress or egress from a highway.

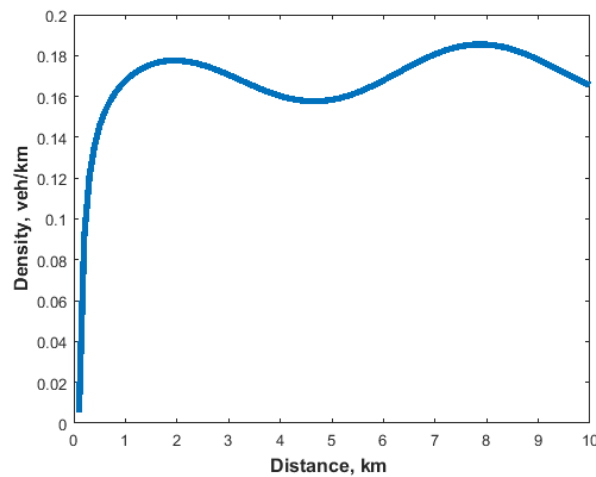


Figure 12. The proposed model density behavior at the ingress to a ramp from a highway at 60 s.

Figure 12 shows the normalized density behavior of the proposed model at the ingress to a ramp from a highway at 60 s. At 0.1 km, the density is 0.010 veh/km, increases to 0.178 veh/km at 1.8 km, and then decreases to 0.158 veh/km at 4.6 km. The density increases to 0.182 veh/km at 7.9 km/ and decreases to 0.165 veh/km at 10 km. Figure 13 presents the corresponding behavior at the egress from a ramp to a highway at 60 s. At 0 km, the density is 0.152 veh/km and decreases to 0.093 veh/km at 1.5 km. It then decreases to 0.074 veh/km at 4.7 km, increases to 0.088 veh/km at 7.9 km, and then decreases to 0.079 veh/km at 10 km. Figure 14 shows the density behavior with the LWR model at the ingress or egress from a highway at 60 s. At 0.1 km, the normalized density is 0.177 veh/km and increases to 0.190 veh/km at 1.5 km. The density decreases to 0.163 veh/km at 4.7 km. The density increases to 0.190 veh/km at 7.8 km and decreases to 0.170 veh/km at 10 km.

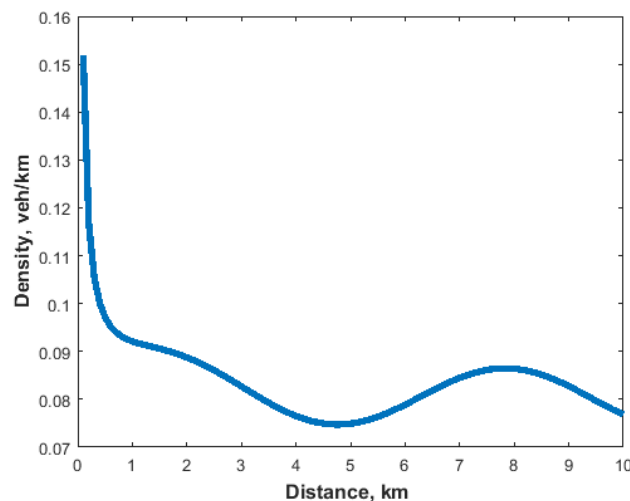


Figure 13. The proposed model density behavior at the egress from a ramp to a highway at 60 s.

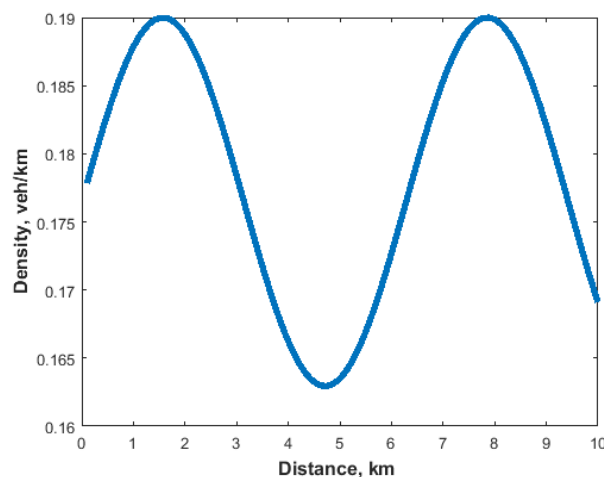


Figure 14. The density behavior at 60 s with the LWR model at the ingress or egress from a highway.

5.1. Traffic Behavior with a 20% Change in Density at 5 km

To further compare the performance of the proposed and LWR models, a situation is considered in which the density is suddenly increased or decreased by 20% at 5 km. Figure 15 shows the proposed model density behavior with a 20% increase in density at 5 km. The density at 0 km is 0.010 veh/km and increases to 0.210 veh/km at 3.5 km. It then decreases to 0.190 at 10 km. Figure 16 shows the LWR model density behavior with a 20% increase in density at 5 km. The density at 0 km is 0.055 veh/km and increases to 0.059 veh/km at 1.5 km. It then decreases to 0.051 veh/km at 5 km. There is a sudden increase in density to 0.061 veh/km at 5 km and it is 0.071 veh/km at 7.9 km. The density then decreases to 0.063 veh/km at 10 km. Figure 17 presents the density behavior with a 20% decrease in density at 5 km. At 0 km, the density is 0.120 veh/km and decreases to 0.076 veh/km at 1 km. It then decreases to 0.059 veh/km at 4.7 km, increases to 0.070 veh/km at 7.9 km, and then decreases to 0.061 veh/km at 10 km. Figure 18 shows LWR model density behavior with a 20% decrease in density at 5 km. The density at 0 km is 0.054 veh/km and increases to 0.059 veh/km at 1.5 km. It then decreases to 0.051 at 5 km and to 0.041 veh/km at 5 km. The density then increases to 0.047 veh/km at 7.9 km and decreases to 0.042 veh/km at 10 km.

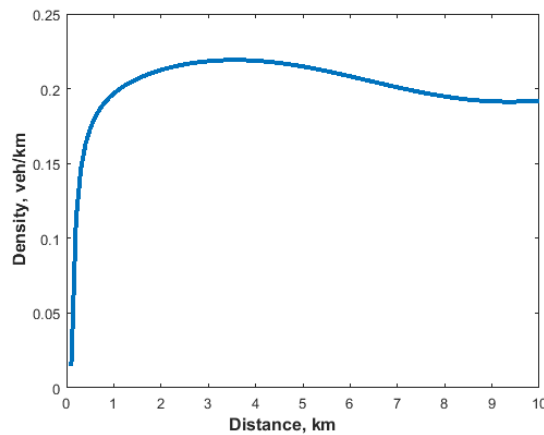


Figure 15. Density behavior of the proposed model with a 20% increase in density at 5 km.

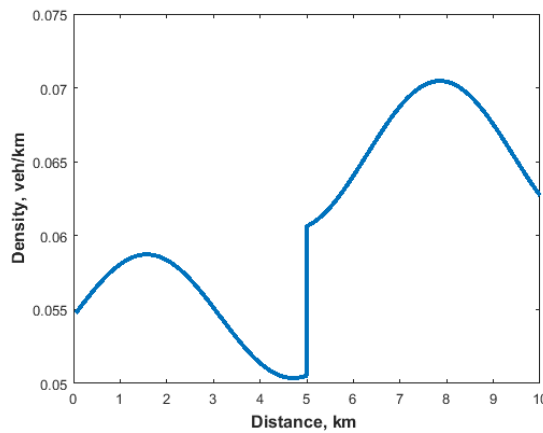


Figure 16. Density behavior of the LWR model with a 20% increase in density at 5 km.

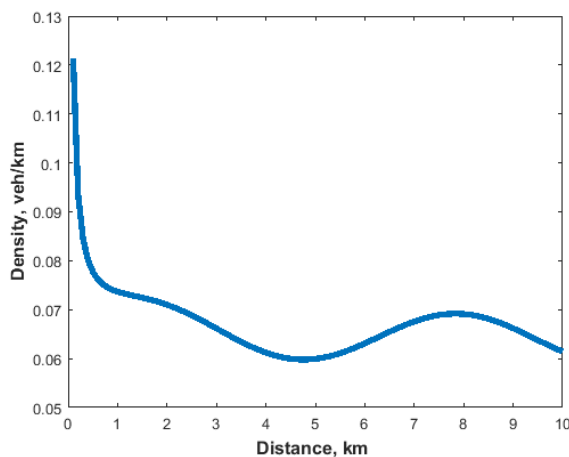


Figure 17. Density behavior of the proposed model with a 20% decrease in density at 5 km.

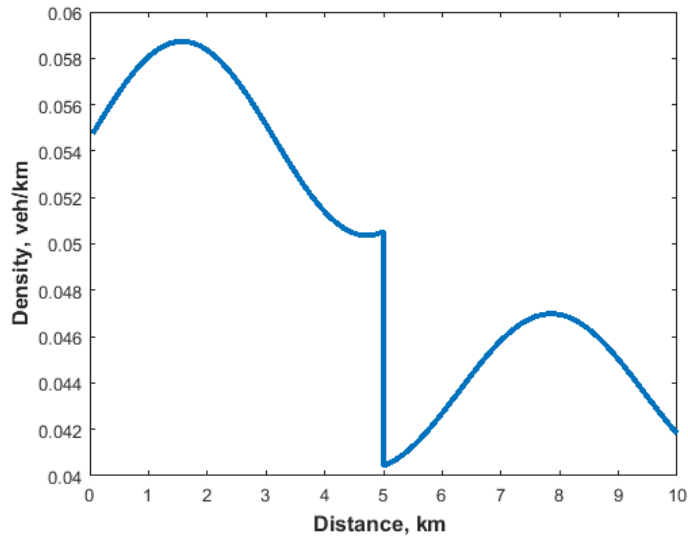


Figure 18. Density behavior of the LWR model with a 20% decrease in density at 5 km.

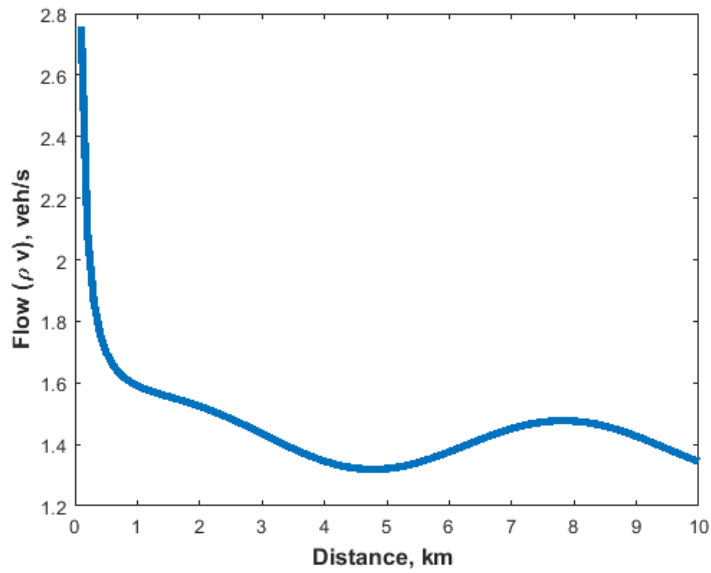


Figure 19. The proposed model traffic flow behavior with a 20% decrease in density at 40 s.

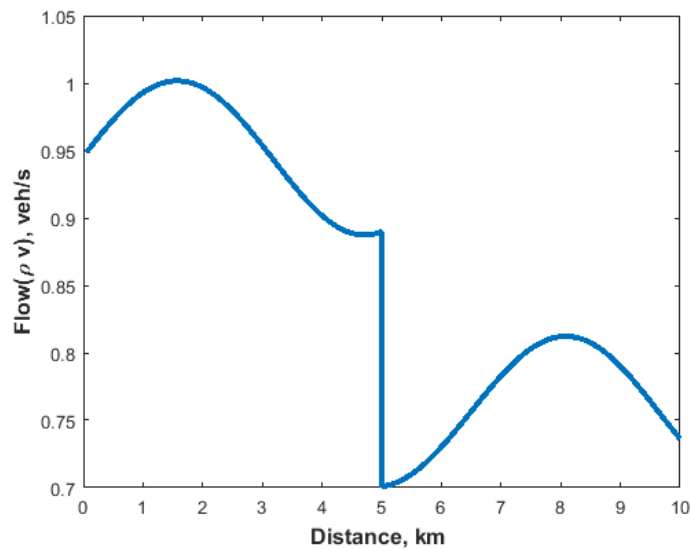


Figure 20. The traffic flow behavior at 40 s with the LWR model with a 20% decrease in density at 5 km.

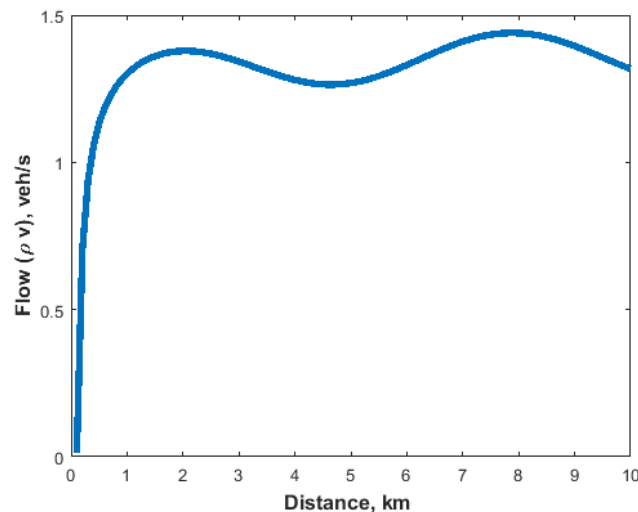


Figure 21. The proposed model traffic flow behavior with a 20% increase in density at 40 s.

5.2. Traffic Flow Comparison

In this section, traffic flow with the proposed and LWR models for a 20% change in density at 5 km is compared. Figure 19 shows the normalized traffic flow behavior of the proposed model with a 20% decrease in density at 40 s. At 0.1 km, the flow is 2.76 veh/s and decreases to 1.60 veh/s at 0.75 km. It further decreases to 1.34 veh/s at 4.7 km, increases to 1.46 veh/s at 7.8 km, and then decreases to 1.33 veh/s at 10 km. Figure 20 shows the LWR model traffic flow behavior at 40 s with a 20% decrease in density at 5 km. The flow at 0 km is 0.90 veh/s, which increases to 1.00 veh/s at 1.5 km. It then decreases to 0.89 veh/s at 4.9 km, which then decreases to 0.70 veh/s at 5 km. The flow increases to 0.81 veh/s at 7.9 km and then decreases to 0.74 veh/s at 10 km. Figure 21 shows the traffic flow behavior of the proposed model with a 20% increase in density at 40 s. At 0.1 km, the flow is 0.100 veh/s and then increases to 1.46 veh/s at 1.5 km. It decreases to 1.29 veh/s at 4.7 km, increases to 1.47 veh/s at 7.8 km, and then decreases to 1.32 veh/s at 10 km.

Figure 1 gives the proposed model density behavior at 1 s for traffic entering a ramp from the highway and Figure 2 provides the corresponding behavior for traffic moving from the ramp towards the highway. For the proposed model, Figures 3, 6, 9 and 12 show the traffic density ingress behavior to a bottleneck when exiting from a highway to a ramp and Figures 4, 7, 10 and 13 show the density egress behavior from a bottleneck at a ramp to a highway. Figures 5, 8, 11 and 14 show the corresponding traffic density behavior with the LWR model. In Figures 1 and 2, there is a slight initial change in density but it is similar for traffic moving towards and away from the ramp. After 10 s the proposed model shows a difference in density profile, but the LWR model shows no difference in traffic behavior. At 20, 50 and 60 s, the traffic density varies over the 10 km road with the proposed model, but not with the LWR model. This indicates that the proposed model can characterize bottleneck behavior better than the LWR model, and this is due to the use of traffic parameters. The proposed model behavior varies according to whether the traffic is entering the ramp from a highway as shown in Figures 1, 3, 6, 9 and 12 or enters the highway from a ramp as shown in Figures 2, 4, 7, 10 and 13. Conversely, the density with the LWR model shown in Figures 5, 8, 11 and 14 is the same regardless of the situation. Thus, the LWR model is unable to characterize changes in traffic density. This is further illustrated in Figures 15, 16, 17 and 18. Figures 15 and 17 show that the proposed model can characterize traffic when there is a sudden change in density. However, the LWR model results in Figures 16 and 17 show an abrupt change in density in both cases which is not realistic. The corresponding traffic flow with the proposed model is shown in Figures 19 and 21. These results indicate that the flow prediction (characterization) with the proposed model is smooth throughout the transition while the LWR model results have abrupt changes in flow as shown in Figure 20. This is because it does not employ parameters such as transition width and driver behavior which are included in the proposed model.

6. Conclusion

In this paper, a new model was proposed to characterize traffic flow behavior at the ingress to or egress from bottlenecks. This model is based on driver reaction and traffic stimuli. Driver reaction is a function of time headway and can be sluggish, typical or aggressive. Traffic stimuli is a function of the transition width and equilibrium velocity and so can be used to characterize traffic behavior due to changes in density. The proposed model reduces to the LWR model when there is no stimulus. The explicit upwind difference scheme was used to evaluate the Lighthill, Whitham, and Richards (LWR) and proposed models with a continuous injection of traffic into the system. Further, a stability analysis of these models was given.

The proposed and LWR models were evaluated over a road of length 10 km which has a bottleneck. Two scenarios were considered, namely traffic from a highway to a ramp (ingress) and from a ramp to a highway (egress). The traffic density was shown to increase at the ingress to a bottleneck and decrease at the egress from a bottleneck. It was shown that the proposed model provides more accurate results in both scenarios because the LWR model cannot characterize traffic adequately when transitions occur. Moreover, sudden changes in traffic with the LWR model produce unrealistic results whereas the results with the proposed model are smooth. Thus, the proposed model is more accurate in both scenarios. The traffic flow profile with this model had no abrupt changes, while the corresponding results with the LWR model were not smooth. The results presented in this paper indicate that the proposed model can be employed at bottlenecks to realistically predict traffic for long and short term planning and in intelligent transportation systems. The LWR model is unsuitable for these purposes.

7. Funding

This project was funded by the Higher Education Commission, Pakistan under the National Centre of Big Data and Cloud Computing at the University of Engineering and Technology, Peshawar, Pakistan.

8. Conflicts of Interest

The authors declare no conflict of interest.

9. References

- [1] INRIX traffic scorecard. Available Online: <http://inrix.com/scorecard/> (Accessed on 10 Apr 2019)
- [2] About traffic indices at this website. Available online: https://www.numbeo.com/traffic/indices_explained.jsp (accessed on 22 April 2019).
- [3] TomTom traffic index. Available Online:http://www.tomtom.com/en_gb/gntrafficindex/. (Accessed on 11 Sep 2018).
- [4] Congestion costs U.K. nearly £ 8 billion in 2018. Available Online:<http://inrix.com/press-releases/scorecard-2018-uk/>. (Accessed on: 10 Apr 2019).
- [5] P. Varaiya, "What we've learned about highway congestion." *Access Magazine* 27 (September 2005):1–9. doi: <https://escholarship.org/uc/item/31j7k3b4>.
- [6] Z. H. Khan, "Traffic modelling for intelligent transportation systems." Ph.D. dissertation, University of Victoria, Victoria, BC, 2016.
- [7] Z. H. Khan and T. A. Gulliver, "A macroscopic traffic model for traffic flow harmonization." *European Transport Research Review* 10 (June 2018):1–12. doi: 10.1186/s12544-018-0291-y.
- [8] Daganzo, Carlos F. "A Behavioral Theory of Multi-Lane Traffic Flow. Part I: Long Homogeneous Freeway Sections." *Transportation Research Part B: Methodological* 36, no. 2 (February 2002): 131–158. doi:10.1016/s0191-2615(00)00042-4.
- [9] Y. Han and S. Ahn, "Stochastic modeling of breakdown at freeway merge bottleneck and traffic control method using connected automated vehicle." *Transportation Research Part B* 107 (February 2018):146–166. doi: 10.1016/j.trb.2017.11.007.
- [10] T. T. Qiao, H. H. Jun, S. C. Wong, G. Z. You and Z. Ying, "A new macro model for traffic flow on a highway with ramps and numerical tests." *Communications in Theoretical Physics* 51 (January 2009):71–78. doi: 10.1088/0253-6102/51/1/15.
- [11] C. A. O'Flaherty, *Transport Planning and Traffic Engineering*, second edition. (January 2006).
- [12] Khan, Zawar H., and T. Aaron Gulliver. "A Macroscopic Traffic Model Based on Anticipation." *Arabian Journal for Science and Engineering* 44, no. 5 (January 30, 2019): 5151–5163. doi:10.1007/s13369-018-03702-9.
- [13] Shvetsov, Vladimir, and Dirk Helbing. "Macroscopic Dynamics of Multilane Traffic." *Physical Review E* 59, no. 6 (June 1, 1999): 6328–6339. doi:10.1103/physreve.59.6328.
- [14] A. Farina, A. Graziano, F. Mariani, M. C. Recchioni and F. Zirilli, "Homogeneous and heterogeneous traffic of data packets on complex networks: The traffic congestion phenomenon." *Communications and Network* 4 (May 2012):157–182. doi:10.4236/cn.2012.42021.
- [15] W. Jin, "Traffic flow models and their numerical solutions." M.S. thesis, University of California Davis, Davis, CA, 2000.
- [16] F. van Wageningen-Kessels, H. van Lint, K. Vuik and S. Hoogendoorn, "Genealogy of traffic flow models." *European Journal of Transport Logistics* 4 (January 2015):445–473. doi: 10.1007/s13676-014-0045-5.
- [17] J. N. Bosire, J. K. Sigey, J. A. Okelo and J. Okwoyo, "Zhang's second order traffic flow models and its application to the Kisii-Kisumu highway within Kisii country." *International Journal of Science and Research* 4 (April 2015):3341–3344.
- [18] H. M. Zhang, "Driver memory, traffic viscosity and a viscous vehicular traffic flow model." *Transportation Research Part B: Methodological* 37 (October 2001):27–41. doi:10.1016/s0191-2615(01)00043-1.

- [19] H. Yu and M. Kristic, "Traffic congestion control for Aw–Rascle–Zhang model." *Automatica* 100 (September 2019):38–51. doi: 10.1016/j.automatica.2018.10.040.
- [20] J. Z. Chen, Z. Shi and Y. Hu, "Numerical solutions of a multi-class traffic flow model on an inhomogeneous highway using a high-resolution relaxed scheme." *Frontiers of Information Technology & Electronic Engineering* 13 (February 2017):1338–1355. doi: 10.1631/jzus.C10a0406.
- [21] D. Helbing and M. Treiber, "Gas-kinetic-based traffic model explaining observed hysteretic phase transition." *Physical Review Letters* 81 (October 1998):3042–3045. doi: 10.1103/PhysRevLett.81.3042.
- [22] A. Kotsialos, M. Papageorgiou, C. Diakaki, Y. Pavlis and F. Middelham, "Traffic flow modeling of large-scale motorway networks using the macroscopic modeling tool METANET." *IEEE Transactions on Intelligent Transportation Systems* 3 (December 2002):282–292. doi: 10.1109/TITS.2002.806804.
- [23] T. Nagatani, "The physics of traffic jams." Ph.D. dissertation, Department of Mechanical Engineering, Shizuoka University, Shizuoka, Japan, 2003.
- [24] D. Vikram, P. Chakroborty and S. Mittal, "Exploring the behavior of LWR continuum models of traffic flow in presence of shock waves." *Procedia - Social and Behavioral Sciences* 104 (December 2013):412–421. doi: 10.1016/j.sbspro.2013.11.134.
- [25] P. Zhang, R. Liu, S. C. Wong and S. Dai, "Hyperbolicity and kinematic waves of a class of multi-population partial differential equation." *Europe Journal of Applied Mathematics* 17 (June 2006):171–200. doi: 10.1017/S095679250500642X.
- [26] E. A. Edison, "Modelling vehicle traffic flow with partial differential equation." B.Sc. thesis, Department of Mathematics, Presbyterian University College, Abetifi, Ghana, 2016.
- [27] N. H. Gartner, C. J. Messer and A. K. Rathi, *Traffic Flow Theory: A State of the Art Report*. Committee on Traffic Flow Theory and Characteristics. (January 2001).
- [28] H. Greenberg, "An analysis of traffic flow." *Operations Research* 7 (August 1958):79–85. doi: 10.1287/opre.7.1.79.
- [29] Z. H. Khan, T. A. Gulliver, H. Nasir, A. Rehman and K. Shahzada, "A macroscopic traffic model based on driver physiological response." *Journal of Engineering Mathematics* 10 (June 2019):1–12. doi: 10.1007/s10665-019-09990-w.
- [30] I. Yperman, S. Logghe and B. Immers, "The link transmission model: An efficient implementation of the kinematic wave theory in traffic networks." *Advanced OR and AI Methods in Transportation* 39 (January 2005):122–130.
- [31] A. Spiliopoulou, M. Kontorinaki, M. Papageorgiou and P. Kopelias, "Macroscopic traffic flow model validation at congested freeway off-ramp areas." *Transportation Research Part C* 41(January 2015):18–29. doi: /10.1016/j.trc.2014.01.009.
- [32] A. Ali, L. S. Andallah and Z. Hossain, "Numerical solution of a fluid dynamic traffic flow model associated with a constant rate inflow." *American Journal of Computational and Applied Mathematics* 5 (January 2015):18–26.
- [33] D. M. Causon and C. G. Mingham, *Introductory Finite Difference Methods for PDEs*. New York, NY: Ventus Publishing, (January 2010):223–227.
- [34] W. L. Jin, "Nonstandard second-order formulation of the LWR model." *Transportmetrica B: Transport Dynamics* 7 (January 2016):1338–1355. doi: 10.1080/21680566.2019.1617.
- [35] R. Marzouga, H. Echab and H. Ez-Zahraouy, "Car accidents induced by a bottleneck." *European Physical Journal B* 90 (December 2017):1–7. doi: 10.1140/epjb/e2017-70695-5.
- [36] M. Badhrudeen, V. Ramesh and L. Vanajakshi, "Headway analysis using automated sensor data under Indian traffic conditions." *Transportation Research Procedia* 17 (December 2016):331–339. doi: 10.1016/j.trpro.2016.11.103.
- [37] H. Khan, Zawar, Waheed Imran, Sajid Azeem, Khurram S. Khattak, T. Aaron Gulliver, and Muhammad Sagheer Aslam. "A Macroscopic Traffic Model Based on Driver Reaction and Traffic Stimuli." *Applied Sciences* 9, no. 14 (July 17, 2019): 2848. doi:10.3390/app9142848.
- [38] W. Imran, Z. H. Khan, T. A. Gulliver, K. S. Khattak and H. Nasir, "A macroscopic traffic model for heterogeneous flow." *Chinese J. Physics* 63 (January 2020):419–435. doi: 10.1016/j.cjph.2019.12.005.
- [39] Z. H. Khan, T. A. Gulliver, K. Azam and K. S. Khattak, "Macroscopic model on driver physiological and psychological behavior at changes in traffic," *J. Eng. Appl. Sci.* 38 (May 2019):1–9. doi: 10.25211/jeas.v38i2.3150.
- [40] Z. H. Khan, T. A. Gulliver, K. S. Khattak and A. Qazi, "A macroscopic traffic model based on reaction velocity." *Iranian Journal of Science and Technology, Transactions of Civil Engineering* 38 (May 2019):1–9. doi: 10.1007/s40996-019-00266-y.
- [41] Z. H. Khan, A. Sullehri, T.A. Gulliver and W. Imran, "On the route choice." *Pakistan Journal Of Science* 38 (December 2019):212–215.
- [42] Z. H. Khan, S. A. A. Shah and T. A. Gulliver. "A macroscopic traffic model based on weather conditions." *Chinese Physics B* 27 (July 2018):1–8. doi: 10.1088/1674-1056/27/7/070202.